Establishment of a bioluminescent MDA-MB-231 cell line for human triple-negative breast cancer research

KE WANG[1], SIMEI XIE[1], YU REN[1], HAIBIN XIA[2], XINWEI ZHANG[1] and JIANJUN HE[1]

[1]Department of Surgical Oncology, First Hospital of Xi'an Jiaotong University, Xi'an 710061;
[2]Laboratory of Gene Therapy, Shaanxi Normal University, Xi'an 710062, P.R. China

Received December 15, 2011; Accepted February 17, 2012

DOI: 10.3892/or.2012.1742

Abstract. The aim of this study was to establish a bioluminescent MDA-MB-231 cell line stably expressing luciferase and green fluorescent protein for the generation of a xenografted model of human triple-negative breast cancer (TNBC) in nude mice. Lentivirus vectors carrying *eGFP*, firefly *luc2* and *neo* fusion genes were used to transduce the MDA-MB-231 human TNBC cells *in vitro*. After 8 weeks of G418 selection, eGFP and luc2 expression was determined using a fluorescence microscope and a Xenogen IVIS200 bioluminescent imaging system, respectively. The MTT, transwell invasion and wound healing assays were performed to confirm whether cellular proliferation, invasion and migration were altered by lentiviral infection. Cells were orthotopically implanted into female BALB/c nude mice to test the sensitivity and stability of reporter gene expression. Growth of the tumors was monitored with the *in vivo* imaging system once a week until they were large enough for experiments. The tumor tissues were resected for histology, and cancer cells were harvested for culture. The lentivirus-transduced MDA-MB-231 cells could stably express luc2 and eGFP, and the luciferase activity reached 9689 photons/sec/cell. Meanwhile, no significant difference in biological activities was observed between the lentivirus-transduced MDA-MB-231 cells and parental cells. An orthotopically implanted tumor model of human TNBCs was successfully established in BALB/c nude mice. Lentiviruses may be ideal carriers for luciferase genes due to their highly efficient infectivity and stable transgene expression. The modified MDA-MB-231 cell line stably expressing luciferase could be detected, allowing for immediate and sensitive detection of metastasis sites in nude mice. As the *eGFP* and *luc2* combination are superior to single reporter genes in their ability to mark cells *in vivo* and *in vitro*, these cells may provide a visualizable, convenient and sensitive platform for research on the mechanisms of metastasis and the development of new antitumor drugs for human TNBC.

Correspondence to: Dr Jianjun He, Department of Surgical Oncology, First Hospital of Xi'an Jiaotong University, 1 Jiankang Road, Xi'an 710061, P.R. China
E-mail: xjtu_wet@163.com

Abbreviations: BLI, bioluminescent imaging; DMEM, Dulbecco's modified Eagle's medium; ER, estrogen receptor; eGFP, enhanced green fluorescent protein; luc2, enhanced firefly luciferase; FBS, fetal bovine serum; Her2, human epidermal growth factor receptor; MTT, 3-(4,5-dimethylthiazol-2-yl)-2,-5-diphenyltetrazolium bromide; PR, progesterone receptor; TNBC, triple-negative breast cancer

Key words: bioluminescent imaging, MDA-MB-231, triple-negative breast cancer, nude mice, implanted tumor model

Introduction

Triple-negative breast cancer (TNBC) cells lack the expression of estrogen receptor (ER), progesterone receptor (PR) and human epidermal growth factor receptor 2 (Her2). Historically, these immunohistochemical markers were commonly used to predict patient prognosis or effects of anti-hormone or anti-Her2 therapies. However, since the notion of a molecular phenotype in breast cancer was brought forth by Perou *et al* (1) in 2000, these three important markers have been used in combination as an immunohistochemical criterion for the molecular classification of breast cancers. Accordingly, breast cancers are divided into three subtypes: the luminal subtype with positive ER expression but negative Her2 expression, the Her2-positive subtype with Her2 overexpression and the triple-negative subtype with the absence of all these markers. Since then, TNBC has become a focus of breast cancer research. Although its morbidity is extremely low, this type of breast cancer is associated with the worst prognoses and lacks an efficient target for therapy (1,2). The poor prognoses of TNBC patients mostly originate from high frequencies of distant organ metastasis, especially brain and viscera metastasis. The mortality rate of TNBC patients with brain metastasis is nearly as high as 100% in the first 3 months of the metastasis (3-5). The outcome of TNBC patients can be greatly improved if the high metastatic capacity of TNBC cells, especially to the brain, can be efficiently eliminated by 'targeted' therapy. Therefore, the main task for researchers of TNBC is to uncover the mechanism accounting for its high propensity to metastasize to the brain and potential targets for TNBC therapy.

As breast cancer mouse models can provide consistent primary mammary tumors and metastasis to clinically relevant tissues such as lymph nodes, lungs, bones and brain, they can be adopted in preclinical evaluations of therapies

for human breast cancer. The objective of this study was to establish in nude mice a model of metastatic brain TNBC, which can be easily and non-invasively detected. Such a model can be used in mechanistic studies of brain metastasis of TNBC. Currently, bioluminescent imaging (BLI) is one of the most widely used techniques to track target cells *in vivo*. Because this technique is based on the fluorescent signal of the chemical reaction between the luciferase and its substrate (D-luciferin), it is highly specific and sensitive. When cancer cells expressing luciferase are inoculated in nude mice by injecting D-luciferin into mice, the fluorescent signal can be detected using a highly sensitive, cooled charge coupled device (CCD) camera mounted in a light-tight specimen box (IVIS™; Xenogen), which allows for quantitation, visualization and real-time monitoring of widespread metastasis in the same breast cancer mouse models over time without harm to the animal (6). In this study, we established and validated a human TNBC cell line that could stably express enhanced firefly luciferase (luc2) and enhanced green fluorescent protein (eGFP) that would be highly valuable for *in vivo* studies of TNBC brain metastasis.

Materials and methods

Cell culture, plasmids and experimental animals. The human breast cancer cell line MDA-MB-231 was obtained from the American Type Culture Collection and maintained in high glucose Dulbecco's modified Eagle's medium (DMEM), supplemented with 50 U/ml penicillin, 50 U/ml streptomycin and 10% heat-inactivated fetal bovine serum (FBS, Hyclone). Human embryonic kidney 293T cells, packaging plasmid psPAX2, envelope plasmid pVPack-VSV-G and transfer plasmid Lenti/F-luciferase2 (luc2)-T2A-eGFP/neomycin were gifts from Haibin Xia (Shaanxi Normal University, China). BALB/c-nu/nu female nude mice (age, 4-6 weeks; body weight, 16-18 g) were obtained from the Shanghai SLAC Laboratory Co. (Shanghai, China). All mice were maintained in specific pathogen-free conditions. All animal experiments were performed in compliance with protocols approved by the Institutional Animal Care and Use Committee of the Xi'an Jiaotong University, China.

Reagents. DMEM, PBS and FBS were obtained from Hyclone. 3-(4,5-dimethylthiazol-2-yl)-2,-5-diphenyltetrazolium bromide (MTT) was from Amresco and Geneticin (G418) was from Invitrogen. The luciferase substrate D-luciferin was purchased from Xenogen. The main instruments included the IVIS200 imaging system (Xenogen IVIS200), an inverted fluorescence microscope (Olympus I X71) and an inverted microscope (Nikon TS100).

Determination of the minimal lethal concentration of G418. After MDA-MB-231 cells were grown to 90% confluence, they were trypsinized and resuspended in complete medium at a density of 1000 cells/ml. One hundred microliters of the cell suspension was added to each well of a 96-well plate. Subsequently, cells were exposed in octuplicate wells to different concentrations of G418 (100, 200, 300, 400, 500, 600, 700, 800, 900, 1000, 1100 and 1200 μg/ml). The minimal concentration of G418 which killed all cells within 14 days was used as the working concentration for selection of infected MDA-MB-231 cells.

Packaging and purification of the lentiviral vector carrying luc2, eGFP and neo fusion genes. 293T cells were split into 150-mm plates and allowed to grow to 50-70% confluence. The old medium was replaced with DMEM containing 2% FBS 1 h before the recombinant plasmid, packaging plasmid and membrane plasmid were co-transfected into the prepared 293T cells by using the calcium-phosphate co-precipitation transfection method. Four hours later, the medium was replaced with DMEM containing 10% FBS, and the culture supernatants of the transfected cells collected at 24, 48 and 72 h after co-transfection were filtered through 0.45 μm membranes to remove cell debris. The filtered supernatants were then centrifuged for 10 min at 1000 rpm, 4˚C, and transferred to a new tube and centrifuged again at 7400 x g, 4˚C, for 16 h to precipitate the virus. The virus pallet was resuspended in DMEM with 2% FBS and directly used for MDA-MB-231 infection.

Virus infection and selection of cells. MDA-MB-231 cells in the exponential phase of growth were harvested and seeded in a 24-well plate at a density of $2x10^3$ cells/well. When the cells grew to 60-70% confluence the following day, the old medium was replaced with 2% FBS DMEM, and the virus suspension was added at three different volumes of 50, 100 or 200 μl. Polybrene was then added into the mixture media at a final concentration of 10 μg/ml. Cells were incubated in the polybrene-medium solution for 24 h and then replaced with fresh complete media. The efficiency of infection was determined by the expression level of eGFP under an inverted fluorescence microscope. Forty-eight hours later, cells with higher expression levels of eGFP were trypsinized and cultured in a new 60-mm plate with selective medium that contained the minimal lethal concentration of G418. The level of G418 was adjusted according to number of eGFP-positive cells. When eGFP expression was stable, positive clones were marked, and 1 μl trypsin was used to detach the cell for 1 sec, and the cell suspension was quickly aspirated for expansion. This procedure was repeated if the cell culture was not pure. The final clonal cell population was selected for 8 weeks and designated as MDA-MB-231-eGFP-luc2.

Evaluation of luciferase activity and its stability in the MDA-MB-231-eGFP-luc2 cell line. MDA-MB-231-eGFP-luc2 cells in the exponential phase of growth were harvested and re-suspended in growth medium at a density of $1x10^5$ cells/ml. The cell suspension was then serially diluted 2-fold ranging from $5x10^4$ to $0.02x10^4$ cells/ml. Cell suspensions (100 μl) from different density groups were seeded in a black 96-well plate (Costar, USA) in duplicate wells. Subsequently, 1 μl D-luciferin (15 mg/ml) was added into one set of the duplicate wells, and the wells without addition of the luciferase substrate served as negative controls. After a 1-min incubation at room temperature, the plate was scanned using the IVIS200 system. Imaging and quantification of signals were controlled by the acquisition and analysis software Living Image® (Xenogen). The bioluminescence was calculated as the number of photons per sec and the exposure time was extended to 5 sec.

Luciferase stability in MDA-MB-231-eGFP-luc2 cells was measured by the following two methods: i) MDA-MB-231-eGFP-luc2 cells were cultured in complete DMEM without G418 for 3 months, and the luciferase activity was measured once a month using the IVIS200 system. ii) MDA-MB-231-eGFP-luc2 cells were orthotopically implanted into the right second mammary fat pad of female BALB/c nude mice to generate xenografts. Both the volume and the luciferase activity of the implanted tumor were recorded every week. Regression plots were generated to correlate the bioluminescence with tumor volume. Primary cells from the xenograft were then harvested and cultured *in vitro*. The luciferase activity of the cultured primary cells was measured using the IVIS200 system after purifying the selection with G418.

Cell proliferation analysis by the MTT assay. The difference between the proliferation of MDA-MB-231 and MDA-MB-231-eGFP-luc2 cells was quantified by measurement of the reduction of MTT to produce a dark blue formazan product by viable cells. Both the MDA-MB-231 and MDA-MB-231-eGFP-luc2 cells were harvested, prepared as single cell suspensions, seeded in 96-well culture plates at 2000 cells/200 μl per well and incubated for 7 days. Every 24 h, 9 wells were used for the MTT assay, and a growth curve was created based on the results.

Flow cytometric cell cycle analysis. The cell cycle distribution was assayed, as described by Nusse *et al* (7), using a Becton-Dickinson fluorescence-activated cell scanner and analyzed using the CellCycle MultiCycle System.

Invasion assay. The invasive capacities of the MDA-MB-231 and MDA-MB-231-eGFP-luc2 cells were evaluated by the transwell invasion assay, as described by Hughes *et al* (8).

Migration assay. The wound healing assay was conducted to test cell migration. Cells in the exponential phase of growth were harvested and seeded in a 6-well plate at a density of $5x10^5$ cells/well. Cells were cultured until near 90% confluence before the assay was performed. First, a line was drawn using a marker on the bottom of the dish, and then a sterile 200 μl pipet tip was used to scratch three separate wounds through the cells, moving perpendicular to the line drawn in the step above (Fig. 1). The cells were gently rinsed twice with PBS to remove floating cells and incubated in 1.5 ml of DMEM medium containing 1% FBS in 37˚C, 5% CO_2 environment. Images of the scratches were taken by using a inverted microscope at x10 magnification at 0 and 24 h of incubation.

Establishment of an orthotopically implanted tumor model in BALB/c nude mice. The MDA-MB-231-eGFP-luc2 and MDA-MB-231 cells were harvested, centrifuged at 1000 rpm for 3 min and then resuspended in 1:1 PBS and matrigel mixtures at a density of $2x10^7$ cells/ml. After being completely anesthetized by 4% chloral hydrate, the mice were immobilized on the left lateral position. Each cell resuspension (100 μl) was orthotopically implanted in the right second mammary fat pad of the mice, as previously described by Kim and Price (9). During the operation, the injection was carefully performed to avoid leakage, and the surgical incision was sutured.

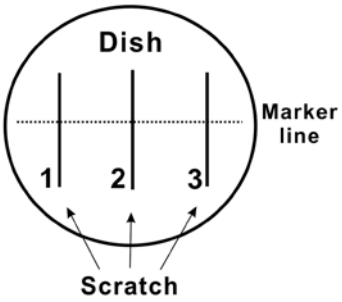

Figure 1. Illustration of wound healing assay.

Evaluation of growth of tumor cells at the primary site of implantation. The lengths and widths of the tumors were measured weekly using a slide caliper when the implanted tumors became megascopic. The volumes were calculated using the formula $V=\pi LW^2/6$. The tumor growth curve (volume vs. time in weeks post-implantation) was constructed for evaluation of the capacity of the cells to generate tumors.

Bioluminescent image analysis. From the day of cell implantation, the growth status of the subcutaneously implanted cells was examined weekly for 4 weeks by BLI using the IVIS200 imaging system. D-luciferin (200 μl of 15 mg/ml solution) was injected into the abdominal cavities of the mice. The nude mice were placed into the chamber for imaging after they were completely anesthetized with a mixture of oxygen and isoflurane. BLI was completed in no more than 15 min after the injection of fluorogenic substrate reagent. The exposure time was set to 5 sec. The parameters of imaging and exposure were kept constant for each measurement. Image signals were analyzed using the Living Image® software (Xenogen). The growth status of the subcutaneously implanted cells was depicted by a tumor-growth curve (fluorescence value per unit area of tumor vs. time in weeks post-implantation).

Pathological examination of implanted tumors. Four weeks after implantation, the animals were sacrificed by cervical dislocation. Tumor tissues were collected and divided into two halves. One half was used to make frozen sections for inspection of eGFP expression, while the other half was embedded in paraffin for analysis by hematoxylin and eosin (H&E) staining. Additional tumor tissues were collected from the mice implanted with MDA-MB-231-eGFP-luc2 cells for primary cell culture.

Primary culture of tumor cells from mice implanted with MDA-MB-231-eGFP-luc2 cells. After being harvested using sterile techniques, each tumor tissue was rinsed with Hanks' solution several times to remove the attached connective tissue and minced into small pieces (<1 mm) with sterile eye scissors. The minced tissue was placed in 0.05% type II collagenase containing medium (1 g tissue/10 ml medium), incubated at 37˚C for ~30 min and digested again with 0.1% trypsin for an additional 15 min. DMEM with 10% FBS was added to the plate to terminate the digestion. The cell suspension was centrifuged at 1000 rpm for 3 min, and then the resuspended

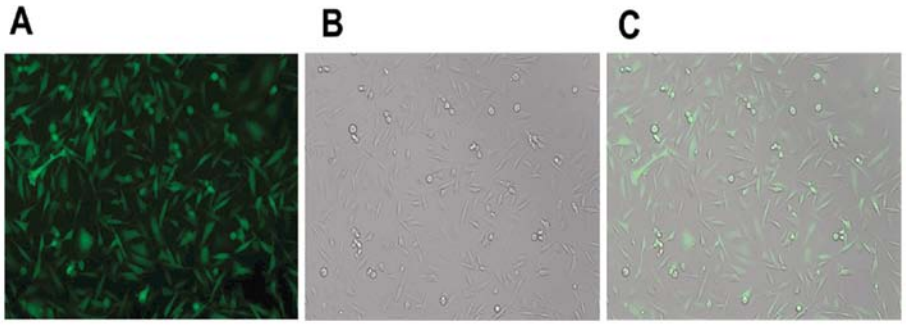

Figure 2. Expression of eGFP in MDA-MB-231-eGFP-luc2 cells (x100). (A) Fluorescence microscopic image; (B) white light microscopic image; (C) merged image of (A) and (B).

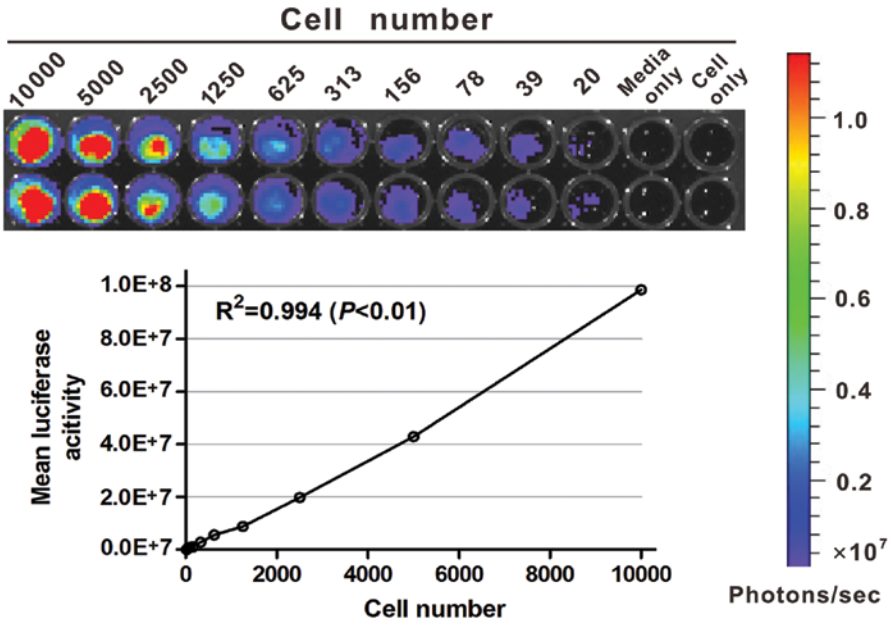

Figure 3. Correlation of bioluminescence intensity with cell quantity in cultured MDA-MB-231-eGFP-luc2 *in vitro*.

cells were cultured in complete DMEM. G418 was added into the growth media to remove mesenchymal cells.

Statistical analysis. Statistical analyses were performed using SPSS 13.0 for Windows. All data were presented as means ± SD, and the Student's t-test was used to compare differences between different groups. P<0.05 was considered statistically significant. Regression plots were used to describe the relationship between bioluminescence and cell number or tumor volume. R^2 values are reported to assess the quality of the regression model.

Results

Selection of stable cell lines. eGFP was observed in all three groups of MDA-MB-231-eGFP-luc2 cells 24 h after infection with three different volumes of lentivirus stock (50, 100 or 200 μl). The group infected with 200 μl of the virus showed the highest fluorescence intensity among the three groups. The fluorescent signal appeared uniformly in the whole cell, and the infection efficiency of this group reached almost 100%. Therefore, virus 200 μl/well was taken as the working concentration in this study, and we took cells from this group for further selection. Forty-eight hours after the infection, the cells were transferred to a 60-mm dish and cultured in cell growth medium with G418 (800 μg/ml) for the selection of positive clones. After 8 weeks of continous selection, eGFP was

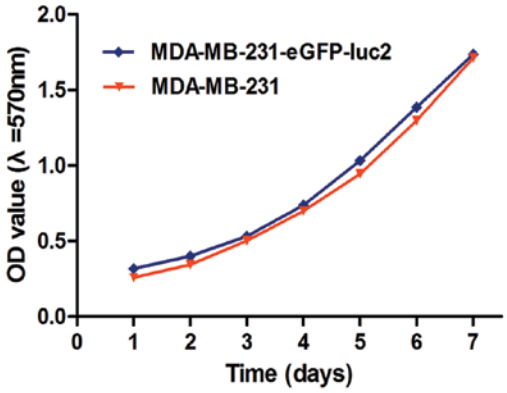

Figure 4. Proliferation curves of MDA-MB-231-eGFP-luc2 and MDA-MB-231 cells show no significant difference.

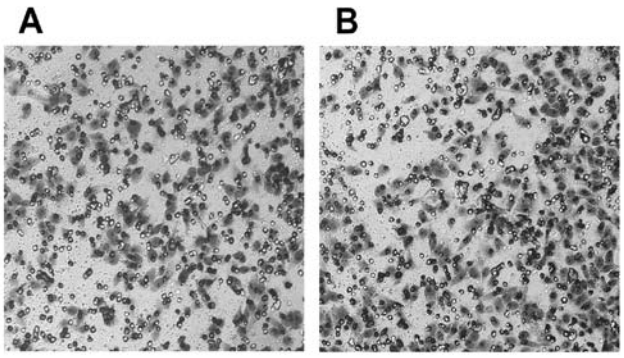

Figure 5. Invasion ability of (A) MDA-MB-231-eGFP-luc2 and (B) MDA-MB-231 cells *in vitro*.

expressed in nearly 100% of the selected cells, and the expression level remained steady during long-term culture (Fig. 2). This stable cell line was named MDA-MB-231-eGFP-luc2.

High and stable expression of luc2 in MDA-MB-231-eGFP-luc2 cells in vitro. The luciferase activity of MDA-MB-231-eGFP-luc2 *in vitro* was measured using the IVIS200 system. The average value of the luciferase activity was up to 9689 photons/sec/cell, and the minimum number of cells detected by the system was 20. In serial 2-fold dilutions of the suspension of MDA-MB-231-eGFP-luc2 cells, the average florescent values of the cell groups significantly correlated with cell numbers (R^2=0.994) (Fig. 3). This stable cell line was then cultured in G418 free medium, and the luciferase activities were measured once a month for 3 months. There was no significant difference between the bioluminescence measured at various time points (data not shown), suggesting that luc2 could be expressed at a stable level by the MDA-MB-231-eGFP-luc2 cell line in long-term culture.

Biological activities of MDA-MB-231-eGFP-luc2 and MDA-MB-231 cells are not significantly different. A series of experiments, including the MTT, transwell invasion and wound healing assays, were performed to confirm whether the main cellular characteristics such as proliferation, invasion and migration had been altered by lentivirus infection. As shown in Fig. 4 and Table I, the modified and parental MDA-MB-231 cells shared similar proliferation curves and cell cycle distributions. The small differences in the proliferation curve and the cell cycle distribution between the two cell lines may be attributed to minor errors in the input of the cell number. In the invasion assay, MDA-MB-231 and MDA-MB-231-eGFP-luc2 cells were allowed to invade for 22 h. At the end of the incubation, membranes were fixed in formalin and stained with 2.5% crystal violet. The stain was eluted using glacial acetic acid, and the absorbance was read at 620 nm. The breast cancer cells, observed under an inverted microscope, were uniformly distributed on the membranes (Fig. 5). The optical density (OD) values for MDA-MB-231-eGFP-luc2 and MDA-MB-231 were 0.886±0.046 and 0.871±0.056, respectively, and not statistically different (P>0.05). In the migration assay, the migration distance was calculated according to the formula mentioned in the methods section. MDA-MB-231-eGFP-luc2 and MDA-MB-231 showed the same average migration distance of 253.33±5.77 μm (Fig. 6). We concluded that the random integration of lentivirus into the genome did not impact the invasion and migration abilities of the MDA-MB-231 cells.

Table I. Cell cycle progression of MDA-MB-231-eGFP-luc2 and MDA-MB-231 cell lines (%).

Cell type	G_0/G_1	S	G_2/M
MDA-MB-231-eGFP-luc2	54.22±1.12	30.48±2.67	15.30±1.71
MDA-MB-231	56.22±2.39	29.27±3.44	13.42±1.89
P-value	>0.05	>0.05	>0.05.

Similar tumorigenicity of MDA-MB-231-eGFP-luc2 and MDA-MB-231 cells in vivo. The orthotopically implanted

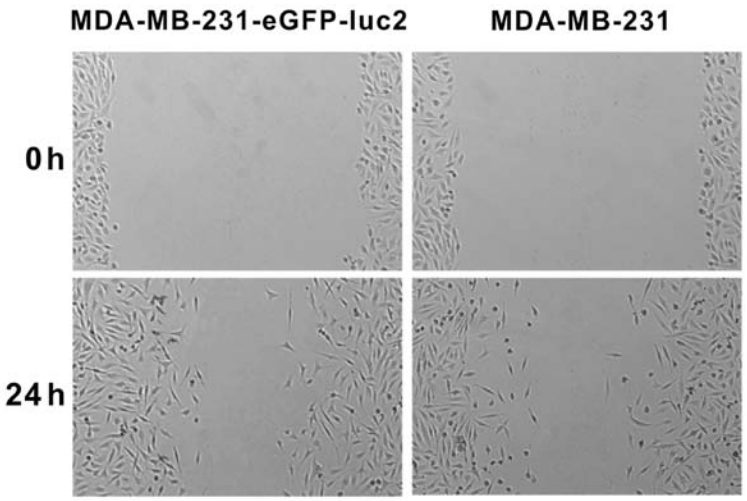

Figure 6. Migration ability of MDA-MB-231-eGFP-luc2 and MDA-MB-231 cells *in vitro* (x50).

Table II. Orthotopic mammary fat pad tumor volumes at different times.

Cell type	Volume (mm^3)			
	1 week	2 weeks	3 weeks	4 weeks
MDA-MB-231-eGFP-luc2	50.572±2.637	61.243±6.395	115.346±8.092	207.912±10.839
MDA-MB-231	51.383±3.082	61.100±5.060	113.385±3.425	202.101±7.420

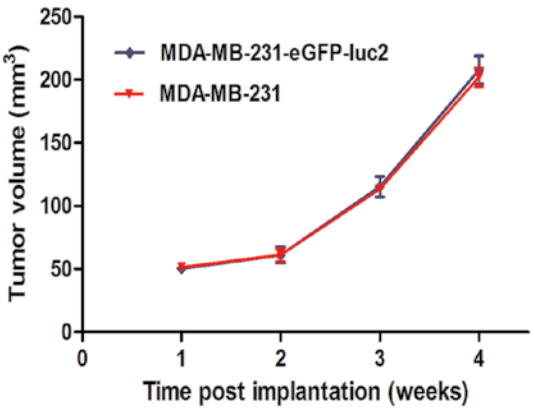

Figure 7. Orthotopic tumor growth curve of MDA-MB-231-eGFP-luc2 and MDA-MB-231 cells.

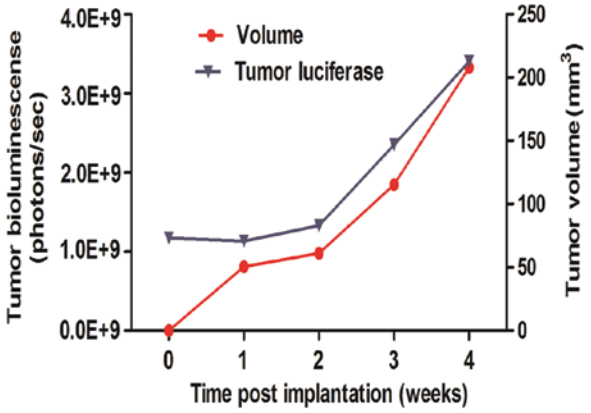

Figure 9. Correlation between bioluminescense intensity and volume of tumors derived from MDA-MB-231-eGFP-luc2 cells.

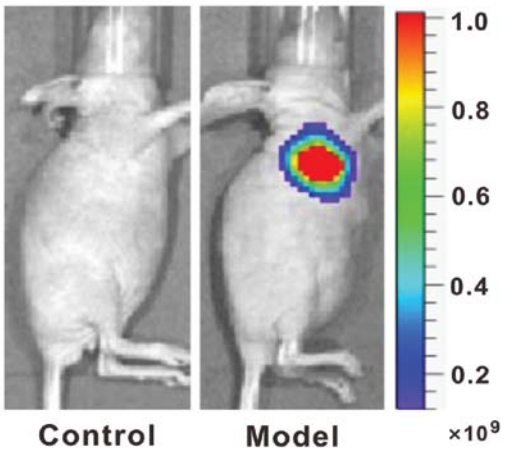

Figure 8. *In vivo* bioluminescence of the orthotopic mammary fat pad after cell injection (week 0). (A) Control mice; (B) experimental mice.

Table III. Volume and bioluminescence of tumors derived from MDA-MB-231-eGFP-luc2 cells at different times.

Time (week)	Volume (mm^3) mean ± SD	Bioluminescence (photons/sec); mean ± SD
0	0	$1.172x10^{10}$±$2.193x10^{9}$
1	50.572±2.637	$1.131x10^{10}$±$3.081x10^{9}$
2	61.243±6.395	$1.328x10^{10}$±$2.458x10^{9}$
3	115.346±8.092	$2.349x10^{10}$±$1.137x10^{9}$
4	207.912±10.839	$3.403x10^{10}$±$3.432x10^{9}$

tumor model was successfully established in 9 nude mice, except for 1 failure due to the outleakage of implanted cells at the primary injection site. All mice were immediately imaged after recovering from surgery. The first BLI test showed an obvious 'hotspot' at the primary location of implantation (Fig. 8). This result indicated that most of the cells were injected into the target area correctly, and that no visible outleakage or diffusion of cell suspension occurred.

Subcutaneous nodules appeared at the primary injection site in all nude mice 7 days after inoculation and continued to grow in a spherical pattern. From the eighth day on, the length and width of the tumor were measured weekly using a slide caliper. The volume of the tumor was calculated using the formula mentioned in the methods section (Table II). The growth curves of tumors generated from the MDA-MB-231-eGFP-luc2 and MDA-MB-231 cells were very similar (Fig. 7). Four weeks after implantation, the nude mice were sacrificed by cervical dislocation, and tumor tissues were separated from the mammary fat pads for pathological analysis and primary cell culture. The H&E staining analysis demonstrated that there was no significant difference in tissue morphology between the tumors derived from MDA-MB-231-eGFP-luc2 and wild-type MDA-MB-231 cells (Fig. 11). Additionally, the morphological features of the tumor-separated MDA-MB-231-eGFP-luc2 cells were similar to those of the parent MDA-MB-231-eGFP-luc2 and wild-type MDA-MB-231 cells under microscopic observation. Thus, compared with the wild-type MDA-MB-231 cell line, MDA-MB-231-eGFP-luc2 showed no significant change in tumorigenicity *in vivo*.

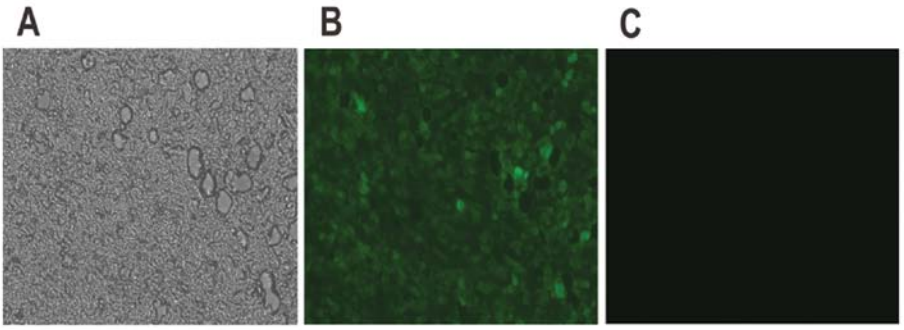

Figure 10. Cryosections of the orthotopic mammary fat pad tumors (10 μm, x200). (A) White light microscopic image; (B) fluorescence microscopic image of MDA-MB-231-eGFP-luc2 tumor; (C) fluorescence microscopic image of MDA-MB-231 tumor.

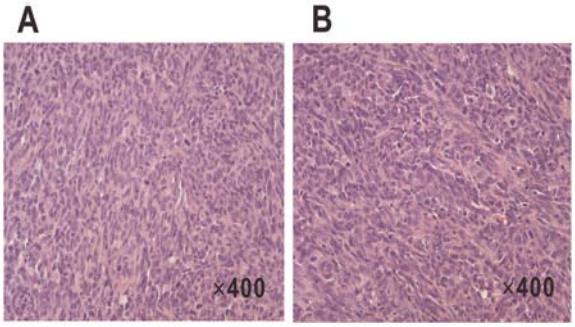

Figure 11. H&E staining of the orthotopic mammary fat pad tumors (x400) (A) MDA-MB-231-eGFP-luc2 tumor; (B) MDA-MB-231 tumor.

Sustainability and consistency of luc2 and eGFP expression in MDA-MB-231-eGFP-luc2 cells in vivo. From the first day of inoculation, BLIs were taken weekly for four weeks until the fluorescence intensity of the implanted tumor cells reached the maximum value. The fluorescence intensity at the primary implantation site generally showed an increasing trend similar to that of the tumor volume (Table III and Fig. 9). In other words, the luciferase activity was significantly correlated with the tumor volume in nude mice (R^2=0.947). When the MDA-MB-231-eGFP-luc2 implanted tumors were seperated for cryosectioning and primary cell culture, eGFP could be observed in the tumor tissues (Fig. 10) as well as the primary cultured cells. By fluorescence microscopy, the expression level of eGFP in the separated MDA-MB-231-eGFP-luc2 cells was observed to be roughly similar to that of the parent MDA-MB-231-eGFP-luc2 cells. In addition, when the primary cultured cells were tested for luciferase activity, the result was not different from that of the parental MDA-MB-231-eGFP-luc2 cells (data not shown). Therefore, both the eGFP and luc2 genes were stably expressed *in vivo*.

Discussion

The basal-like breast cancer subtype is characterized by a gene expression profile that is similar to that of the basal epithelial or myoepithelial layer of the normal mammary duct. As described above, this subgroup of breast cancers are the TNBC-type that lack expression of ER, PR and HER2 (10). Since being identified, TNBC has attracted increasing attention from oncologists due to its relatively poor clinical outcome and lack of molecules for targeted therapies. It has been reported that the prognosis for patients having TNBC is worse than those with HER2 overexpressing breast cancer (3,4). The main reason for its poor prognosis is thought to be the high rate of brain or viscera metastasis, and patients with such metastasis will die within a short period of time after diagnosis (3-5,11,12). Based on the clinical metastatic characteristics of TNBC, the objective of this study was to establish a xenograft model of human brain metastatic TNBC cells in nude mice for the investigation of molecular mechanisms underlying the high propensity of TNBC cells to transfer to the brain and for the detection of potential molecular targets for treatment of brain metastatic cancers. The successful establishment of a brain metastatic TNBC model in nude mice depends on whether a platform is available to permit non-invasive, quantitative, visualizable and real-time monitoring of the development of brain metastases. Fortunately, newly-developed *in vivo* optical imaging technologies, including the BLI system and the fluorescence imaging system, can provide such a platform, which will ensure that animals are euthanized at the right time point to obtain a sufficient number of metastatic tumor samples for a given experiment.

The *in vivo* optical imaging technique has become an indispensable method in a number of research applications, including monitoring of transgene expression and progression of infection, transplantation, toxicology, virology, tumor growth and metastasis, and exploration of new antitumor drug and gene therapies (13). This technique, which has the advantage of being visualizable, non-invasive and easy to carry out, has been used widely in the developed countries, and various commercialized tumor cell lines marked with the *luc* gene, *GFP* gene or their combination have been established for tumor research *in vivo*. However, this technique is still immature in China. According to published articles, only two breast cancer cell lines, MCF-7 and ZR-75-1, have been constructed for *in vivo* optical imaging research, and neither of them is a TNBC cell line (14). In this study, the MDA-MB-231-eGFP-luc2 cell line, which could be detected by BLI in nude mice, was constructed using the typical human TNBC cell line MDA-MB-231 (15).

Some problems still exist in the establishment of stable cell lines that are available for optical imaging in China. First, most cells are marked with a single reporter gene such as *GFP* or *luc*. The main difference between the two techniques is that

the former uses an external light source to excite the GFP, while for the latter, the light is naturally emitted by cells that have been genetically labeled by the *luc* gene. As the animal's hair and skin can also produce non-specific fluorescence when stimulated by an external light source, the signal-to-noise-ratio in fluorescence imaging is lower than that in BLI. Compared to fluorescence imaging, BLI is more appropriate for *in vivo* research due to its higher sensitivity, specificity and capacity for quantitive analysis, while the GFP-based fluorescence imaging is more suitable for *in vitro* experiments due to the ease of visual detection using a fluoroscope. As these two techniques have different sensitivity limits and advantages, we recommend the combined application of both reporter genes. In addition, most available cell lines are marked with the first generation *GFP* or *luc* gene. Compared to the new generation reporter genes *eGFP* and *luc2* (16), the first generation *GFP* and *luc* exhibit relatively low activity and require more than 100 cells for *in vitro* detection (17). Under this circumstance, a larger number of tumor cells is needed to improve the sensitivity of *in vivo* imaging, which will not only increase the tumor burden of the animal but also increase the likelihood of death from embolism if a high number of tumor cells is injected into the circulation (18).

In this study, we avoided the disadvantages discussed above by using lentiviruses carrying the *luc2*, *eGFP* and *neo* fusion genes to transduce the human TNBC cell line MDA-MB-231. The results showed that the *eGFP* and *luc2* genes were stably expressed both *in vitro* and *in vivo* at high levels, and that the activity of luc2 reached 9689 photons/sec/cell *in vitro*, which was far higher than the 100-148 photons/sec/cell reported by Jenkins *et al* (19). The high activities of the *eGFP* and *luc2* genes facilitated detection of the micrometastases *in vivo*. Although producing an appropriate luciferase/eGFP-expressing cell line for *in vivo* optical research requires an investment of time, both the selection and evaluation processes are important. First, the biological characteristics of the cells may be affected by lentiviruses, which are randomly integrated into the host cell genome (20). Thus, the potential effects of lentiviral infection on proliferation, invasion and migration abilities of MDA-MB-231 cells as well as the stability of reporter gene expression required evaluation. Injection of cells with altered characteristics and unstable expression of reporter genes into mice would yield unreliable results. We found no significant differences in the biological activities between the lentivirus-infected MDA-MB-231-eGFP-luc2 cells and the parental cells. Therefore, the established MDA-MB-231-eGFP-luc2 cell line is suitable for application in the brain metastastic TNBC model in nude mice.

In addition to permitting non-invasive, quantitative and real-time visualizable monitoring of the development of metastases in small animals, the eGFP and luc2 double-labeled tumor cells can be used as a supplemental tool in many experiments. For example, the double-labeled tumor cells can be used to verify whether implantation is successful in the process of establishing metastatic animal models, especially when injections are made in the left ventricle. Generally, the cancer cell distribution in the whole body can be shown by the fluorescent images obtained with the Xenogen IVIS200 BLI system 2 h after the injection. If the signals are distributed over the entire body, the injection is considered successful, whereas if the signals are limited to the heart or lung area, the cells may have been incorrectly injected into the right ventricle or may have leaked into the thoracic cavity. With the application of the imaging system, a failed animal model can be eliminated at an early time point, thus avoiding unnecessary waste of time and resources. The double-labeled tumor cells can also enable the *in vitro* experiments to be conveniently conducted, as eGFP can be directly observed by an inverted fluoroscope. In this study, this technique was successfully used to evaluate the virus transduction efficiency and to select eGFP positive cells. Furthermore, the fluorescent signals, which reflect the sensitive and specific chemical reaction between the luciferase and its substrate (luciferin), can be used to indirectly predict the number of cancer cells. Thus, this technique is highly useful for multiple *in vitro* experiments and assays, such as cell adhesion/migration/invasion assays and cell proliferative activity/drug suppressive experiments (21).

In conclusion, our results demonstrated that lentivirus vectors may be ideal as carriers of luciferase genes due to their highly efficient infectivity and ability to generate stable transgene expression. The combination of two reporter genes is superior to single reporter genes in the ability to mark cells *in vitro* and *in vivo*. The MDA-MB-231-eGFP-luc2 cell line established in our study is suitable for producing a brain metastatic TNBC mouse model. Combination of the implanted tumor cells in nude mice and the BLI technique provides an intuitionistic and reliable platform for research on the mechanism of tumor cell metastasis and evaluation of antitumor effects of targeted therapy. Importantly, the animal model established using luciferase-expressing cancer cells detectable by BLI provides a system for non-invasive, real-time and quantitative analysis of tumor biomass and metastasis.

References

1. Perou CM, Sorlie T, Eisen MB, van de Rijn M, Jeffrey SS, Rees CA, Pollack JR, Ross DT, Johnsen H, Akslen LA, *et al*: Molecular portraits of human breast tumours. Nature 406: 747-752, 2000.
2. van't Veer LJ, Dai H, van de Vijver MJ, He YD, Hart AA, Mao M, Peterse HL, van der Kooy K, Marton MJ, Witteveen AT, *et al*: Gene expression profiling predicts clinical outcome of breast cancer. Nature 415: 530-536, 2002.
3. Ihemelandu CU, Naab TJ, Mezghebe HM, Makambi KH, Siram SM, Leffall LD, DeWitty RL and Frederick WA: Basal cell-like (triple-negative) breast cancer, a predictor of distant metastasis in African American women. American J Surg 195: 153-158, 2008.
4. Sørlie T, Tibshirani R, Parker J, Hastie T, Marron JS, Nobel A, Deng S, Johnsen H, Pesich R, Geisler S, *et al*: Repeated observation of breast tumor subtypes in independent gene expression data sets. Proc Natl Acad Sci USA 100: 8418-8423, 2003.
5. Abd El-Rehim DM, Ball G, Pinder SE, Rakha E, Paish C, Robertson JFR, Macmillan D, Blamey RW and Ellis IO: High-throughput protein expression analysis using tissue microarray technology of a large well-characterised series identifies biologically distinct classes of breast cancer confirming recent cDNA expression analyses. Int J Cancer 116: 340-350, 2005.
6. Jenkins D, Oei Y, Hornig Y, Yu S, Dusich J, Purchio T and Contag P: Bioluminescent imaging (BLI) to improve and refine traditional murine models of tumor growth and metastasis. Clin Exp Metastasis 20: 733-744, 2003.
7. Nusse M, Beisker W, Hoffmann C and Tarnok A: Flow cytometric analysis of G1- and G2/M-phase subpopulations in mammamlian cell nuclei using side scatter and DNA content measurement. Cytometry 11: 813-821, 1990.
8. Hughes L, Malone C, Chumsri S, Burger A and McDonnell S: Characterisation of breast cancer cell lines and establishment of a novel isogenic subclone to study migration, invasion and tumourigenicity. Clin Exp Metastasis 25: 549-557, 2008.

9. Kim LS and Price JE: Clinically relevant metastatic breast cancer models to study chemosensitivity. Methods Mol Med 111: 285-295, 2005.
10. Cleator S, Heller W and Coombes RC: Triple-negative breast cancer: therapeutic options. Lancet Oncol 8: 235-244, 2007.
11. Kennecke H, Yerushalmi R, Woods R, Cheang MCU, Voduc D, Speers CH, Nielsen TO and Gelmon K: Metastatic behavior of breast cancer subtypes. J Clin Oncol 28: 3271-3277, 2010.
12. Dent R, Hanna W, Trudeau M, Rawlinson E, Sun P and Narod S: Pattern of metastatic spread in triple-negative breast cancer. Breast Cancer Res Treat 115: 423-428, 2009.
13. Sadikot RT and Blackwell TS: Bioluminescence imaging. Proc Am Thorac Soc 2: 537-540, 2005.
14. Li Y, Zhang HY, Wang Z and Zhang BL: Establishment of an animal model of breast cancer based on in vivo bioluminescence imaging. Tumor 29: 76-80, 2009 (In Chinese).
15. Cailleau R, Young R, Olivé M and Reeves WJ Jr: Breast tumor cell lines from pleural effusions. J Natl Cancer Inst 53: 661-674, 1974.
16. Kim J, Urban K, Cochran E, Lee S, Ang A, Rice B, Bata A, Campbell K, Coffee R, Gorodinsky A, *et al*: Non-invasive detection of a small number of bioluminescent cancer cells. PLoS One 5: e9364, 2010.
17. Minn AJ, Gupta GP, Siegel PM, Bos PD, Shu W, Giri DD, Viale A, Olshen AB, Gerald WL and Massague J: Genes that mediate breast cancer metastasis to lung. Nature 436: 518-524, 2005.
18. Hakim F, Fowler DH, Shearer GM and Gress RE: Animal models of acute and chronic graft-versus-host disease. Curr Protoc Immunol 4: 4.3.1-4.3.21, 2001.
19. Jenkins D, Hornig Y, Oei Y, Dusich J and Purchio T: Bioluminescent human breast cancer cell lines that permit rapid and sensitive in vivo detection of mammary tumors and multiple metastases in immune deficient mice. Breast Cancer Res 7: R444-R454, 2005.
20. Michel G, Yu Y, Chang T and Yee JK: Site-specific gene insertion mediated by a Cre-loxP-carrying lentiviral vector. Mol Ther 18: 1814-1821, 2010.
21. Vishwanath RP, Brown CE, Wagner JR, Meechoovet HB, Naranjo A, Wright CL, Olivares S, Qian D, Cooper LJN and Jensen MC: A quantitative high-throughput chemotaxis assay using bioluminescent reporter cells. J Immunol Methods 302: 78-89, 2005.